

Charge ordering in the spinels AlV_2O_4 and LiV_2O_4

Y. Z. Zhang¹, P. Fulde¹, P. Thalmeier² and A. Yaresko¹

¹Max-Planck-Institut für Physik komplexer Systeme, Nöthnitzer Straße 38 01187 Dresden, Germany

²Max-Planck-Institut für Chemische Physik fester Stoffe, Nöthnitzer Straße 40 01187 Dresden, Germany
(January 25, 2019)

We develop a microscopic theory for the charge ordering (CO) transitions in the spinels AlV_2O_4 and LiV_2O_4 (under pressure). The high degeneracy of CO states is lifted by a coupling to the rhombohedral lattice deformations which favors transition to a CO state with inequivalent V(1) and V(2) sites forming Kagomé and trigonal planes respectively. We construct an extended Hubbard type model including a deformation potential which is treated in unrestricted Hartree Fock approximation and describes correctly the observed first-order CO transition. We also discuss the influence of associated orbital order. Furthermore we suggest that due to different band fillings AlV_2O_4 should remain metallic while LiV_2O_4 under pressure should become a semiconductor when charge disproportionation sets in.

PACS: 71.30.+h; 71.70.-d; 71.10.Fd; 71.20.Be

It was Wigner [1] who first pointed out that electrons form a lattice when the mutual Coulomb repulsion dominates the kinetic energy gain from delocalization. He considered an electron gas with a positive uniform background (jellium). Within that model a lattice will form only when the electron concentration is very low. Detailed calculations have determined the critical concentration below which lattice formation or charge ordering takes place and a value of $r_c \simeq 35a_B$ was found [2]. Here r_c is the critical value of the average distance between electrons which must be exceeded and a_B is Bohr's radius. The conditions for charge ordering of electrons are much better when the uniform, positive background is replaced by a lattice of positive ions. Depending on the overlap of atomic wavefunctions on neighbouring sites the energy gain due to electron delocalization can be rather small and a dominance of Coulomb repulsion is more likely. For a more detailed description see, e.g. [3]. A good example is Yb_4As_3 which exhibits charge order (CO) and for which a microscopic theory was provided [4]. Here Yb $4f$ holes gain a small energy only by delocalizing via As $4p$ hybridization. Another well known example is magnetite Fe_3O_4 , a spinel structure. Verwey and Haayman [5] found a metal-insulator phase transition to occur which they attributed to a charge ordering of the Fe^{2+} and Fe^{3+} sites on the pyrochlore sublattice of the spinel lattice (B-sites). According to Verwey [5] in the charge ordered state the corner-sharing tetrahedra forming the pyrochlore structure are occupied by two Fe^{2+} and two Fe^{3+} ions each. This rule, (tetrahedron rule) was most clearly formulated by Anderson [6] and allows for an exponential number of different configurations. Recently this rule has been questioned by LDA+U calculation [7] which seemingly give good results for the observed charge disproportionations [8] when the low-temperature structure is put into the calculations.

In this investigation we consider AlV_2O_4 [9] and LiV_2O_4 [10,11]. In both systems the V ions form a py-

rochlore lattice. While in AlV_2O_4 a charge order phase transition at approximately 700 K has been observed [9] at ambient pressure, in LiV_2O_4 electronic charge orders only under hydrostatic pressure of approximately 6 GPa [11]. In both cases structural changes are associated with charge ordering. In AlV_2O_4 the lattice distortions change the cubic high-temperature phase into a lattice with alternating layers of Kagomé and triangular planes. They are stacked in [111] direction and formed by nonequivalent V(1) and V(2) sites. The rhombohedral lattice deformation causes an increase in the V(1)-O(1) and V(1)-O(2) bond lengths and a decrease in the V(2)-O(1) bond length. The changes in the distances V(1)-V(1) denoted by L_1 and V(1)-V(2) by L_2 below the phase transition temperature T_{CO} define a deformation $\epsilon(T) = (L_2 - L_1)/L$. L is the V-V distance in the undistorted case. At T = 300 K this value was found to be $\epsilon(300K) = 0.016$. Below T_{CO} the average valence of the V ions changes from +2.5 in the high-temperature phase to $+2.5 - \delta$ at the V(1) sites and to $+2.5 + 3\delta$ at the V(2) sites. This is schematically shown in Fig. 1.

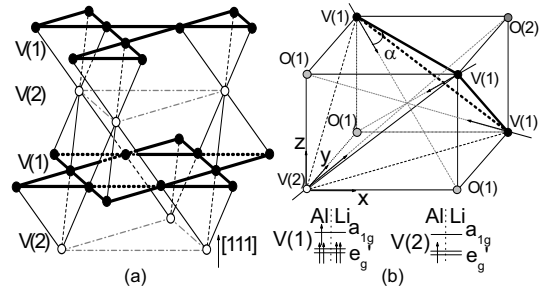


FIG. 1. (a) Sublattice of the V ions. In the presence of a distortion the V(1) sites form a Kagomé and the V(2) sites a triangular lattice. (b) AlV_2O_4 and LiV_2O_4 in the atomic limit. Shown are the splittings of the t_{2g} orbitals, their occupations, the spin vectors and the angle α with respect to the [111] plane.

Also associated with the charge-order transition are a small but steep increase in the resistivity and a pro-

nounced decrease of the magnetic susceptibility. In LiV_2O_4 the lattice distortion connected with the charge order under pressure seems to be similar to that of AlV_2O_4 as powder X-ray diffraction indicate [11]. However the structural parameters have not yet been determined. Due to the different filling of the t_{2g} band AlV_2O_4 seems to remain a semimetal or a small gap semiconductor while LiV_2O_4 is becoming an insulator with a steep increase in the resistivity below the phase transition temperature T_{CO} .

The first thought is to perform for AlV_2O_4 and LiV_2O_4 under pressure LDA+U calculation of the type reported for Fe_3O_4 (see [7]). We have done such calculations for AlV_2O_4 . However, although the LDA+U approach was shown to provide a realistic description of the electronic structure of magnetic insulators, its application to paramagnets is less justified because calculations can only be performed for a magnetically ordered state. In addition, LDA+U is too crude an approximation to reproduce the low energy excitation spectrum of strongly correlated metals and, thus, can hardly be used to study the high temperature metallic phase of AlV_2O_4 and the change of the electronic structure upon heating through the phase transition. For LiV_2O_4 LDA+U calculations are not yet possible since the CO crystal structure under pressure is not known. Therefore we proceed here differently. We want to provide a microscopic Hamiltonian in order to identify the physical process which results in the observed structural phase transition and the accompanying charge order while enforcing a proper nonmagnetic state. The price are adjustable parameters entering the theory for which no ab initio values are available. From standard band-structure calculations it is known that the Fermi energy E_F of V 3d electrons lies within the t_{2g} band which is well separated from the remaining bands. Therefore we only include t_{2g} electrons in the model defined by

$$H = H_0 + H_{int} + H_{e-p} \quad , \text{ with} \quad (1)$$

$$\begin{aligned} H_0 &= \sum_{\langle l\mu, l'\mu' \rangle} \sum_{\langle \langle l\mu, l'\mu' \rangle \rangle \nu\nu' \sigma} t_{\mu\mu'}^{\nu\nu'}(l, l') c_{l\mu\nu\sigma}^+ c_{l'\mu'\nu'\sigma} \\ H_{int} &= \sum_{l\mu} \{ (U + 2J) \sum_{\nu} n_{l\mu\nu\uparrow} n_{l\mu\nu\downarrow} + U \sum_{\nu > \nu'} n_{l\mu\nu\sigma} n_{l\mu\nu'\bar{\sigma}} \\ &+ (U - J) \sum_{\nu > \nu'} n_{l\mu\nu\sigma} n_{l\mu\nu'\sigma} \} + \frac{V}{2} \sum_{\langle l\mu, l'\mu' \rangle \nu\nu' \sigma\sigma'} n_{l\mu\nu\sigma} n_{l'\mu'\nu'\sigma'} \\ H_{ep} &= \varepsilon \Delta \sum_{l\nu\sigma} \sum_{\mu} \left(\delta_{\mu,1} - \frac{1}{3} (1 - \delta_{\mu,1}) \right) n_{l\mu\nu\sigma} + K \sum_l \varepsilon^2 \end{aligned}$$

Here H_0 describes the kinetic energy. The electron creation and annihilation operators are specified by four indices, i.e., for the unit cell (denoted by l), the sublattice ($\mu = 1, 2, 3, 4$), the t_{2g} orbital ($\nu = d_{xy}, d_{yz}, d_{zx}$), and the spin ($\sigma = \uparrow, \downarrow$). The brackets $\langle \dots \rangle$ and $\langle \langle \dots \rangle \rangle$ indicate a summation over nearest-neighbour (n.n.) and next-nearest-neighbour (n.n.n.) sites respectively. The

term H_{int} describes the on-site Coulomb and exchange interactions U and J among the t_{2g} electrons. The last term contains the Coulomb repulsion V of an electron with those on the six neighbouring sites. Finally H_{ep} describes the coupling to lattice distortions. The deformation potential is denoted by Δ , it is due to a shift in the orbital energies of the V sites caused by changes in the oxygen positions relative to the vanadium positions. While the energy shift is positive for the V(1) sites it is negative for the V(2) sites.

The elastic constant K refers to the c_{44} mode and describes the energy due to the rhombohedral lattice deformation. It is reasonable to assume that like in Fe_3O_4 [12] and Yb_4As_3 [13] only the c_{44} mode is strongly coupled with the charge disproportionation. We can give at least approximate values for all parameters except V and Δ . Their ratio will be fixed by the CO transition temperature while keeping the constraint $V \ll U$. For the on-site Coulomb- and exchange integrals we take $U = 3.0$ eV and $J = 1.0$ eV which are values commonly used for vanadium oxides [14]. Band structure calculations which we have performed demonstrate that the hopping matrix elements $t_{\mu\mu'}^{\nu\nu'}$ between different orbitals $\nu \neq \nu'$ are negligible. For simplicity we first ignore them and omit ν, ν' . Then $t = -t_{\mu\mu'}(l, l')$ when l, l' are n.n. and t' for n.n.n.. We will take into account the orbital dependent hopping matrix elements coming from a tight-binding fit of LDA calculations as orbital order is included. Furthermore the c_{44} elastic constant is not known for AlV_2O_4 or LiV_2O_4 , while computational methods for its ab initio calculation in the case of materials with strong electronic correlations are not mature enough. Therefore we use a representative value $c_{44}^{(0)}/\Omega = 6.1 \cdot 10^{11}$ erg/cm³ for AlV_2O_4 where Ω is the volume of the cubic unit cell with a lattice constant of $a = 5.844$ Å. This value is close to the experimental value for Fe_3O_4 which has also the spinel structure. This leads to $K \simeq 1.1 \cdot 10^2$ eV. The deformation potential Δ is not known but is commonly of the order of the band width. For convenience we introduce the dimensionless coupling constant $\lambda = \Delta^2/Kt$ and lattice distortion $\delta_L = \epsilon\Delta/t$. From LDA calculations the bandwidth is $8t = 2.7$ eV, and therefore a reasonable value is $\lambda t = \Delta^2/K = 1$ eV. This means $\Delta = 10.5$ eV which is twice the value of Yb_4As_3 [4]. We begin by considering H_0 only. By transforming to Bloch states $a_{\mathbf{k}\xi\nu\sigma}^+$ we obtain

$$\begin{aligned} H_0 &= \sum_{\mathbf{k}\xi\nu\sigma} \epsilon_{\xi}(\mathbf{k}) a_{\mathbf{k}\xi\nu\sigma}^+ a_{\mathbf{k}\xi\nu\sigma} \quad , \text{ with} \\ \epsilon_{1,2}(\mathbf{k}) &= 2(t - t') \\ \epsilon_{3,4}(\mathbf{k}) &= -2t \left[1 \mp \sqrt{1 + \eta_{\mathbf{k}}} \right] + 2t' \left[1 - 2\eta_{\mathbf{k}} \pm 2\sqrt{1 + \eta_{\mathbf{k}}} \right] \end{aligned} \quad (2)$$

Here $\eta_{\mathbf{k}} = (\cos k_x \cos k_y + \cos k_y \cos k_z + \cos k_z \cos k_x)$. With four V ions per unit cell, three t_{2g} orbitals and two spin directions there are altogether 24 bands, of which

twelve are dispersionless and degenerate ($\epsilon_{1,2}$). In addition there are two sixfold degenerate dispersive bands present ($\epsilon_{3,4}$). The band structure has been considered before [15] and we refer to that reference for more details. The Fermi energy lies in a region of high density of states (DOS) $N(E)$ which depends sensitively on the ratio t'/t .

Next we discuss the effect of the deformation-potential coupling described by H_{ep} . When it is sufficiently strong it may lead to charge order. However, there is no gap opening but only a sharp decrease of DOS around E_F , i.e., the system remains metallic. When we include the U and V terms in mean-field approximation, assuming a paramagnetic state, the results remain qualitatively unchanged. A strong on-site U term suppresses CO while increasing inter-site V term will induce CO. Again there is no gap opening at E_F but a decrease of DOS at the CO transition for all t' . We note that in the present case a n.n.n hopping t' supports CO because it increases $N(E_F)$, while it prevents CO in the half-filled square lattice [16]. Since here $t' \ll t$ has little effect on CO we neglect it for simplicity.

In our calculations we assume a homogeneous deformation along [111] direction. This yields the following relation between the lattice distortion and charge disproportionation

$$\delta_L = \lambda (n_2 - n_1) / 2 \quad (3)$$

where $n_1 = \sum_{\nu\sigma} \langle n_{1\nu\sigma} \rangle$ is the occupation of a V(2) site while $n_2 = n_3 = n_4$ with $n_\mu = \sum_{\nu\sigma} \langle n_{\mu\nu\sigma} \rangle$ is the occupation of a V(1) site.

In any case, the mean-field analysis of the model Hamiltonian (1) leads to a second order phase transition as function of temperature. This is at odds with the experimental observation of a strong first order CO transition. We believe that this is the effect of charge correlations caused by large U and V. To include this effect in a qualitative way, we have treated the model within an unrestricted Hartree-Fock calculation by breaking the magnetic symmetry but preserving the constraint of zero total moment. We assume that the sites μ have an occupation $n_\mu = \sum_{\nu\sigma} \langle n_{\mu\nu\sigma} \rangle$ and a magnetization $m_\mu = \sum_{\nu\sigma} \sigma \langle n_{\mu\nu\sigma} \rangle$. The spins are assumed to be directed towards the center of the tetrahedron in the undistorted phase. In the distorted phase we change the angle α so that the net magnetization remains zero (see Fig. 1 (b)). Because there are two tetrahedra per unit cell translational symmetry is maintained. The free energy is

$$F = -\frac{1}{\beta} \ln \Xi + N_e \mu - \frac{5NU}{12} \sum_\mu n_\mu^2 + \frac{N}{12} (U + 4J) \sum_\mu m_\mu^2 - NV \sum_\mu \sum_{\mu \neq \mu'} n_\mu n_{\mu'} + N \frac{\delta^2}{\lambda} \quad (4)$$

where N is the total number of unit cell and $N_e = 10$ N is the electron number per unit cell. Furthermore Ξ is the grand canonical partition function

$$\ln \Xi = 3 \sum_{\mathbf{k}\xi\sigma} \ln \left[1 + e^{-\beta(\epsilon_\xi^\sigma(\mathbf{k}) - \bar{\mu})} \right] \quad (5)$$

with $\beta = 1/k_B T$. The chemical potential $\bar{\mu}$ is adjusted to yield the correct filling, i.e., $N_e = \frac{1}{\beta} \frac{\partial}{\partial \bar{\mu}} \ln \Xi$. The energy bands $\epsilon_\xi^\sigma(\mathbf{k})$ depend now on spin σ for which the [111] direction is chosen as quantization axis. They are computed by diagonalizing the Hamiltonian (1) in mean-field approximation and by self-consistent determination of n_μ and m_μ from $(\partial F / \partial n_\mu)_{\bar{\mu}} = 0$ and $(\partial F / \partial m_\mu)_{\bar{\mu}} = 0$, respectively at various temperatures T .

With the magnetization pattern described above and shown in Fig. 1 (b) we must transform the nearest-neighbour hopping matrix elements so that the different spin directions are accounted for. We label the electronic spin functions of sublattice 1 by $|\sigma_1\rangle$ and $|\bar{\sigma}_1\rangle$ and those referring to sublattice 2, 3, and 4 by $|\sigma_\mu\rangle$ and $|\bar{\sigma}_\mu\rangle$. We then apply the transformation to a local spin quantization axis

$$\begin{pmatrix} |\sigma_\mu\rangle \\ |\bar{\sigma}_\mu\rangle \end{pmatrix} = \begin{pmatrix} \cos \frac{\theta}{2} & -e^{i\gamma_\mu} \sin \frac{\theta}{2} \\ e^{-i\gamma_\mu} \sin \frac{\theta}{2} & \cos \frac{\theta}{2} \end{pmatrix} \begin{pmatrix} |\sigma_1\rangle \\ |\bar{\sigma}_1\rangle \end{pmatrix} \quad (6)$$

where $\theta = \frac{\pi}{2} + \alpha$ and $\gamma_\mu = 0, \frac{2\pi}{3}, \frac{4\pi}{3}$ for $\mu=2, 3, 4$. All the interaction terms as well as the electron-phonon coupling term remain invariant under this transformation. The angle α is adjusted such that $\sum_\mu m_\mu = 0$ for all distortions.

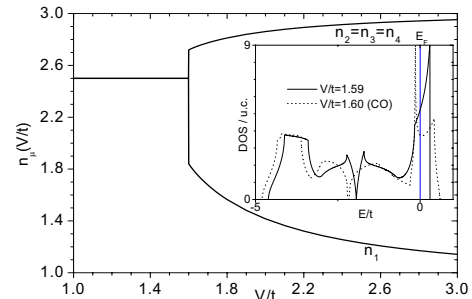


FIG. 2. Charge disproportionation as function of V/t . The n_μ denote the occupation numbers of the four sites of a tetrahedron. In the inset the changes in the density of states are shown when V/t is just below and above the critical value at which charge ordering sets in. At the critical $V/t=1.67$ $n_1=2.5+3\delta$ and $n_i=2.5-\delta$ ($i=2-4$) with a charge disproportionation $\delta \simeq 0.25$. Here $U=3.0\text{eV}$, $J=1.0\text{eV}$, $\lambda t=1.0\text{eV}$ and $8t=2.7\text{eV}$.

The result for the charge disproportionation at $T=0$ as function of the electronic nearest-neighbour Coulomb repulsion V is shown in Fig. 2. As usual the charge disproportionation is larger (by a factor of 2.5 here) than the one obtained from a valence bond analysis of the distorted structure. This is due to the simplified Hamiltonian which cannot describe the screening effects of non-d electrons. The same observation was made for Yb_3As_4 [4]. Also shown as an inset is the change in the DOS for a V value just below and above the critical value at which

charge order does occur. Apparently the DOS changes considerably near E_F due to charge order. This may explain the drop in the susceptibility and the small but steep increase in the resistivity in AlV_2O_4 when charge order sets in. The self-consistent field calculations were done for different temperatures. The phase transition to the distorted phase is found to be of first order. Fixing the value $V/t=1.67$ leads to the calculated transition temperature is $T_c=660$ K in reasonable agreement with the experimental value of $T_c^{\text{exp}}=700$ K. The phase diagram is found to be very simple. For $U=3$ eV, $J=1.0$ eV and $8t=2.7$ eV we find a phase boundary line of the form $\lambda t+3V=7.8t$. For all λt values above that line the trigonal, i.e., distorted phase is found while for values below that line the phase remains cubic.

It is obvious that with a lattice distortion an associated orbital order will occur [17]. The point symmetry in the charge ordered state is D_{3d} and lifts partially the 3-fold degeneracy of the t_{2g} states. This results in one a_{1g} orbital and 2-fold degenerate e'_g orbitals. Experiments show in the distorted phase an elongation in [111] direction and a corresponding contraction perpendicular to that direction. Therefore the orbital energy of the a_{1g} state is expected to be higher than that of the e'_g states.

From the behavior in the atomic limit (see Fig. 1 (b)) we expect that the system remains gapless in the charge ordered state even when orbital order occurs. This is indeed what we find. We have adopted hopping matrix elements which reproduce the LDA band structure. They are $t_0 = t_{14}^{xy,xy} = -0.525$ eV and $t_1 = t_{12}^{xy,xy} = t_{13}^{xy,xy} = 0.152$ eV. The upmost band remains almost flat. By solving self-consistently for the mean-field parameters $n_{\mu\nu}$ and $m_{\mu\nu}$ under the constraint that the occupation numbers of the three V(1) sites remain equal we find that $n_2^{xy} = n_2^{zx} > n_2^{yz}$, $n_3^{xy} = n_3^{yz} > n_3^{zx}$ and $n_4^{yz} = n_4^{zx} > n_4^{xy}$. For simplicity we have used here the notation of the t_{2g} basis. It shows that the orbital orders on sublattices 2, 3 and 4 are perpendicular to each other. At the V(2) sites there is no orbital ordering in the charge ordered phase. Since the system remains gapless and the orbital order does not change the effects induced by charge order and magnetic order, i.e., a sharp decrease of DOS around the Fermi surface and a first-order phase transition respectively, its role is insignificant at 5/12-filling (AlV_2O_4).

Now we compare the above findings with the charge order observed in LiV_2O_4 under pressure. Here the average d electron number per V site is 1.5. The atomic limit shown in Fig. 1 (b) suggests a gap and therefore insulating behavior in the charge ordered phase. This is also what is found when the Hamiltonian (1) is treated in mean-field approximation for 1/4 filling as required for LiV_2O_4 instead of 5/12. The essential role for orbital order and gap formation is played by the different 3d-occupation of LiV_2O_4 therefore we use similar values for hopping terms and interaction strengths are used as for AlV_2O_4 . The DOS at $T=0$ is shown in Fig. 3. The

opening of a gap is in agreement with the behavior of $\rho(T)$ as found in Ref. [11].

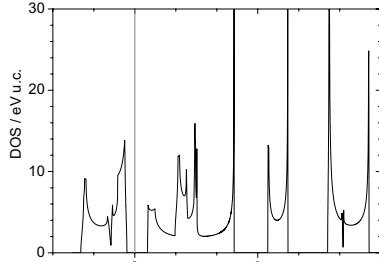


FIG. 3. Density of states in LiV_2O_4 in the distorted phase. It is seen that the system is a semiconductor with a gap $E_g=0.49\text{eV}$. Here $U=3.0\text{eV}$, $J=1.0\text{eV}$, $V=0.7\text{eV}$, $\Delta^2/K=1.0\text{eV}$, $t_0=-0.53\text{eV}$, $t_1=0.15\text{eV}$

In summary, we have provided a microscopic model for the observed charge order in AlV_2O_4 and LiV_2O_4 under pressure which is mainly driven by a deformation potential coupling to t_{2g} states. The model accounts correctly for the observed first order CO transition. We have also shown that due to a difference in the filling factors AlV_2O_4 should remain metallic in the charge ordered phase while LiV_2O_4 should become an insulator or semiconductor.

We thank Drs. G. Venkateswara Pai, T. Maitra, E. Runge and Y. Zhou for helpful discussions.

- [1] E. Wigner, Trans. Faraday Soc. 34, 678 (1938).
- [2] M. Imada and M. Takahashi, J. Phys. Soc. Jpn. 53, 3770 (1984); B. Tanatar and D. M. Ceperley, Phys. Rev. B 39, 5005 (1989).
- [3] Fulde, Ann. Phys. (Leipzig) 6, 178 (1997).
- [4] Fulde, B. Schmidt, and P. Thalmeier, Europhys Lett. 31, 323 (1995).
- [5] E. J. W. Verwey, Nature (London) 144, 327 (1939); E. J. W. Verwey, P. W. Haayman, and F. C. Romeijn, J. Chem. Phys. 15, 181 (1947).
- [6] P. W. Anderson, Phys. Rev. 102, 1008 (1956).
- [7] I. Leonov, A. N. Yaresko, V. N. Antonov, M. A. Korotin, and V. I. Anisimov, Phys. Rev. Lett. 93, 146404 (2004); Horng-Tay Jeng, G. Y. Guo and D. J. Huang, Phys. Rev. Lett. 93, 156403 (2004).
- [8] J. P. Wright, J. P. Attfield, P. G. Radaelli, Phys. Rev. Lett. 87, 266401 (2001).
- [9] K. Matsuno, T. Katsufuji, S. Mori, Y. Moritomo, A. Machida, E. Nishibori, M. Takata, M. Sakata, N. Yamamoto and H. Takagi, J. Phys. Soc. Jpn. 70, 1456 (2001); K. Matsuno, T. Katsufuji, S. Mori, M. Nohara, A. Machida, Y. Moritomo, K. Kato, E. Nishibori, M. Takata, M. Sakata, K. Kitazawa, and H. Takagi, Phys. Rev. Lett. 90, 096404 (2003).
- [10] S. Kondo, D. C. Johnston, C. A. Swenson, F. Borsa, A. V. Mahajan, L. L. Miller, T. Gu, A. I. Goldman, M. B. Maple, D. A. Gajewski, E. J. Freeman, N. R. Dilley, R. P. Dickey, J. Merrin, K. Kojima, G. M. Luke, Y. J. Uemura, O. Chmaissem, and J. D. Jorgensen, Phys. Rev. Lett. 78, 3729 (1997).

- [11] K. Takada, H. Hidaka, H. Kotegawa, T. C. Kobayashi, K. Shimizu, H. Harima, K. Fujiwara, K. Miyoshi, J. Takeuchi, Y. Ohishi, T. Adachi, M. Takata, E. Nishibori, M. Sakata, T. Watanuki, O. Shimomura, in press; H. Ueda, C. Urano, M. Nohara, H. Takagi, K. Kitazawa, N. Takesita, N. Mori, unpublished.
- [12] H. Schwenk, S. Bareiter, C. Hinkel, B. Luethi, Z. Kakol, A. Koslowski, and J. M. Honig, Eur. Phys. J. B 13, 491 (2000).
- [13] T. Goto, Y. Nemoto, A. Ochiai, and T. Suzuki, Phys. Rev. B 59, 269 (1999).
- [14] A. Fujimori, K. Kawakami, and N. Tsuda, Phys. Rev. B 38, R7889 (1988).
- [15] M. Isoda and S. Mori, J. Phys. Soc. Jpn. 69, 1509 (2000).
- [16] M. Vekic, R. M. Noack, and S. R. White, Phys. Rev. B 46, 271 (1992).
- [17] M. Imada, A. Fujimori, and Y. Tokura, Rev. Mod. Phys. 70, 1039 (1998).